Developmental Biology 347 (2010) 195–203

Contents lists available at ScienceDirect

Developmental Biology

journal homepage: www.elsevier.com/developmentalbiology

Growth differentiation factor 11 signaling controls retinoic acid activity for axial vertebral development

Young Jae Lee [a,b,*], Alexandra McPherron [c], Susan Choe [a], Yasuo Sakai [d], Roshantha A. Chandraratna [e], Se-Jin Lee [c], S. Paul Oh [a,b,f,*]

[a] Department of Physiology and Functional Genomics, College of Medicine, University of Florida, Gainesville, FL 32610, USA
[b] Laboratory of Developmental Genetics, Lee Gil Ya Cancer and Diabetes Institute, Gachon University of Medicine and Science, Incheon, Republic of Korea
[c] Department of Molecular Biology and Genetics, Johns Hopkins University School of Medicine, Baltimore, MD 21205, USA
[d] Plastic and Reconstructive Surgery, Fujita Health University, Toyoake, Aichi 470-1192, Japan
[e] NuRx Pharmaceuticals Inc., Irvine, California 92618, USA
[f] World Class University Program, Lee Gil Ya Cancer and Diabetes Institute, Gachon University of Medicine and Science, Incheon, Republic of Korea

ARTICLE INFO

Article history:
Received for publication 20 March 2010
Revised 20 August 2010
Accepted 20 August 2010
Available online 27 August 2010

Keywords:
GDF11
ACVR2
CYP26A1
Retinoic acid
Vertebral patterning
RAR inhibitor

ABSTRACT

Mice deficient in growth differentiation factor 11 (GDF11) signaling display anterior transformation of axial vertebrae and truncation of caudal vertebrae. However, the *in vivo* molecular mechanisms by which GDF11 signaling regulates the development of the vertebral column have yet to be determined. We found that *Gdf11* and *Acvr2b* mutants are sensitive to exogenous RA treatment on vertebral specification and caudal vertebral development. We show that diminished expression of Cyp26a1, a retinoic acid inactivating enzyme, and concomitant elevation of retinoic acid activity in the caudal region of $Gdf11^{-/-}$ embryos may account for this phenomenon. Reduced expression or function of Cyp26a1 enhanced anterior transformation of axial vertebrae in wild-type and *Acvr2b* mutants. Furthermore, a pan retinoic acid receptor antagonist (AGN193109) could lessen the anterior transformation phenotype and rescue the tail truncation phenotype of $Gdf11^{-/-}$ mice. Taken together, these results suggest that GDF11 signaling regulates development of caudal vertebrae and is involved in specification of axial vertebrae in part by maintaining Cyp26a1 expression, which represses retinoic acid activity in the caudal region of embryos during the somitogenesis stage.

Introduction

The vertebral column consists of vertebrae, which protect the spinal cord and provide articulation for movement. Depending on the position and morphological characteristics along the anteroposterior (AP) axis, vertebrae are grouped into cervical, thoracic, lumbar, sacral and caudal vertebrae. The thoracic vertebrae are characterized by the attachment of ribs, and the sacral vertebrae are characterized by the formation of the sacrum. In mammals, from whales to giraffes, the number of cervical vertebrae is invariably seven except for a few species. The number of vertebrae in thoracic, lumbar and sacral regions in mammals is almost invariable within a species but considerably varies between species. For instance, mice have seven cervical (C), thirteen thoracic (T), six lumbar (L), four sacral (S), and over 20 caudal vertebrae, as represented by the C7T13L6S4 vertebral pattern, whereas the human, chimp and horse vertebrae display C7T12L5S5, C7T14L3S5 and C7T18L6S5 patterns, respectively. The vertebral pattern represents the hallmark of the metameric body plan along the AP axis that provides spatial cues for the development of the diaphragm and segmental structures such as the axial muscles, intercostal blood vessels, and projections of spinal nerve systems.

Each vertebra is formed from two adjacent pairs of somites, which also form occipital bones and ribs (Saga and Takeda, 2001). Nascent somites are added to the last segmented somite at a relatively constant rate (about 2 hours in mice) from the presomitic mesoderm (PSM) region, while new mesoderm is concomitantly added at the posterior end of PSM from the tail bud. The manner in which somites acquire their positional information along the AP axis to exhibit their distinctive morphological characteristics has been studied extensively (Baker et al., 2006; Gregg, 2007; Saga and Takeda, 2001). Transplantation experiments in chickens have shown that vertebral specification is established in the PSM region before the segmental plates bud off the PSM and develop into structurally identifiable nascent somites (Nowicki and Burke, 2000). Ample comparative and genetic studies have shown that a specific array of *Hox* genes (a Hox code) is crucial for the specification of a vertebra (Wellik, 2007). Among *Hox* genes, *Hox10* and *Hox11* paralogous genes have been shown to play a role in suppressing rib

* Corresponding authors. Y.J. Lee is to be contacted at Lee Gil Ya Cancer and Diabetes Institute, Gachon University of Medicine and Science, 7-45 Songdo-dong, Yunsu-gu, Incheon, Republic of Korea. Fax: +82 032 899 6414. S.P. Oh, Department of Physiology and Functional Genomics, University of Florida, 1376 Mowry Road, Room 456, Gainesville, FL 32610, USA. Fax: +1 352 273 8300.
E-mail addresses: leeyj@gachon.ac.kr (Y.J. Lee), ohp@ufl.edu (S.P. Oh).

0012-1606/$ – see front matter © 2010 Elsevier Inc. All rights reserved.
doi:10.1016/j.ydbio.2010.08.022

attachments to lumbar and sacral vertebrae and in the formation of the sacrum, respectively (Carapuco et al., 2005; Wellik and Capecchi, 2003). Activities of these *Hox* genes in the PSM, but not in somites, are sufficient for global vertebral patterning (Carapuco et al., 2005). However, the molecular mechanism by which a segmental plate acquires a specific Hox code is poorly understood.

Studies with gain- or loss-of-function mutations in mice have shown that a number of genes are involved in the regulation of multiple *Hox* genes and thereby affect vertebral patterning (Mallo et al., 2009). These genes include the *CDX* family transcription factors (van den Akker et al., 2002), Polycomb group global gene regulators (Akasaka et al., 2001; Core et al., 1997), proteins involved in retinoic acid (RA) synthesis, metabolism, and signaling (Abu-Abed et al., 2001, 2003; Allan et al., 2001; Kessel, 1992; Kessel and Gruss, 1991; Sakai et al., 2001), and proteins involved in GDF11 signaling (Andersson et al., 2006; McPherron et al., 1999; Oh and Li, 1997; Szumska et al., 2008). In this paper we focus on the interactions between RA metabolism and GDF11, two signaling systems involved in vertebral patterning.

Exogenous administration of RA to pregnant females at 8.5 days post coitum (dpc) induces the posterior shift of the Hox code and anterior transformation of vertebrae, resulting in C7/T14/L6 or C7/T15/L5 patterns (Kessel and Gruss, 1991). Homeostasis of RA activity in the caudal region of embryo is essential for the vertebral patterning and the development of caudal vertebrae. In normal mice, RA is inactivated in the caudal region by a cytochrome P450 enzyme, CYP26A1, which catabolizes RA to 4-hydroxy RA (White et al., 1996; Pearlmann, 2002). Repression of RA is essential for the expression of a number of genes, such as *Wnt3a*, *Fgf8* and *bracyury*, in the tail bud region (Abu-Abed et al., 2001, 2003; Sakai et al., 2001). Mice deficient in *Cyp26a1* exhibit markedly elevated RA activity in the tail bud, homeotic transformation of vertebrae, and caudal agenesis (Abu-Abed et al., 2001, 2003; Sakai et al., 2001). Moreover, RA receptor deficiency can rescue the axial vertebral defects of *Cyp26a1*-null mice, demonstrating that elevated RA in the caudal region is the cause of the vertebral defects in *Cyp26a1*$^{-/-}$ mice (Abu-Abed et al., 2003).

GDF11 is a member of the transforming growth factor-β (TGF-β) superfamily and is involved in axial vertebral patterning and development of the palate, kidney, and pancreas (Dichmann et al., 2006; Esquela and Lee, 2003; McPherron et al., 1999). The active form of TGF-β superfamily proteins is generated by proteolytic cleavage of the precursor protein. Recent studies have shown that proprotein convertase PCSK5 (PC5/6) is necessary for the activation of Gdf11 (Essalmani et al., 2008; Seidah et al., 2008; Szumska et al., 2008). The TGF-β family signal is transduced through interactions with heteromeric complexes of type II and type I receptors (Massague, 1998). Activin type II receptors (ACVR2A and ACVR2B) and the TGF-β type I receptor (ALK5; TGFBR1) have been shown to mediate the GDF11 signal for vertebral specification (Andersson et al., 2006; Oh and Li, 1997; Oh et al., 2002). SMAD2 and SMAD3 are known cytoplasmic targets of ACVR2/2B and ALK5 (Massague, 1998; Oh et al., 2002).

Gdf11$^{-/-}$ mice exhibit anterior transformations of the axial skeleton, resulting in an increased number of thoracic and lumbar vertebrae (C7/T18/L8) and truncation of caudal vertebrae (McPherron et al., 1999). GDF11 has functional redundancy with GDF8 (myostation; Mstn) in patterning and development of the axial skeleton (McPherron et al., 2009): most *Gdf11*$^{-/-}$;*Mstn*$^{-/-}$ mice have an increase in severity of anterior transformation (mostly 20 thoracic vertebrae) and tail truncation (up to sacral vertebrae), as compared to *Gdf11*$^{-/-}$ mice. The vertebral transformation defects of *Gdf11*$^{-/-}$;*Mstn*$^{-/-}$ mice represent the most remarkable phenotype among all known vertebral patterning defects of multiple mutant mice in terms of the extent of the transformation. The closest phenotypic resemblance is found in mice with triple *Hox* gene deletion (Wellik and Capecchi, 2003; McIntyre et al., 2007), suggesting that expressions of multiple *Hox* genes are affected in *Gdf11*$^{-/-}$ mice. Consistent with this, it has been demonstrated that the expression boundaries of multiple *Hox* genes are shifted posteriorly in *Acvr2b*$^{-/-}$, *Gdf11*$^{-/-}$, and *Pcsk5*$^{-/-}$ mice (Essalmani et al., 2008; McPherron et al., 1999; Oh and Li, 1997; Szumska et al., 2008). However, the mechanism by which Gdf11 signaling controls multiple *Hox* genes for axial vertebral patterning remains unknown.

In this paper, we present data suggesting that GDF11 signaling is an important determinant for the RA gradient along the AP axis by regulating CYP26A1 expression in the tail bud region for proper vertebral specification and tail development.

Materials and methods

Mouse strains

All mouse strains used in this study are listed as follows: *Gdf11*-, *Acvr2a*-, *Acvr2b*-, *Cyp26a1*-knockout mice, and *RARE-LacZ* transgenic mice (McPherron et al., 1999; Oh and Li, 1997; Rossant et al., 1991; Sakai et al., 2001; Song et al., 1999; Yang et al., 1999). Mice were maintained under standard specific-pathogen-free conditions and all animal procedures performed were reviewed and approved by the University of Florida and Johns Hopkins University School of Medicine Institutional Animal Care and Use Committee.

Mouse mating schemes

For monitoring the *in vivo* RA activity, *Gdf11*$^{+/-}$;*RARE-lacZ(+)* and *Acvr2b*$^{+/-}$;*RARE-lacZ(+)* males were intercrossed with *Gdf11*$^{+/-}$ and *Acvr2b*$^{+/-}$ females, respectively. Embryos were collected at E8.5 and E10.5 for X-gal staining. For genetic interaction between *Acvr2b* and *Cyp26a1*, *Acvr2b*$^{-/-}$ males were intercrossed with *Acvr2b*$^{+/-}$; *Cyp26a1*$^{+/-}$ females, and the vertebral patterns of *Acvr2b*$^{-/-}$; *Cyp26a1*$^{+/-}$ newborn pups were compared with those of *Acvr2b*$^{-/-}$ and *Acvr2b*$^{+/-}$;*Cyp26a1*$^{+/-}$ pups. For the RA sensitivity study, *Acvr2b*$^{-/-}$ males were intercrossed with *Acvr2b*$^{+/-}$;*Acvr2a*$^{+/-}$ females. RA was administered to dams at 8.5 dpc as described below.

Administration of R115866, retinoic acid, and AGN193109

10 mM R115866 (Johnson & Johnson Co.) stock was made in DMSO and the aliquots were stored in −20 °C freezer. The stock solution was diluted in PEG200 just prior to use and administered to pregnant dams at 8.5 dpc via oral gavage needles. All-*trans* RA (Sigma-Aldrich, St. Louis, MO) was dissolved in DMSO at 25 mg/ml and stored at −20 °C in the dark. The RA stock solution was subjected to a 10-fold dilution in sesame oil and orally administrated to the pregnant mice at 8.5 dpc at a final concentration of 10 mg/kg of body weight. AGN193109 (Allergan Inc., Irvine, CA) was dissolved in DMSO at 1 mg/ml and stored at −20 °C freezer. The stock solution was diluted in corn oil just before use and administrated to pregnant dams at 8.5 and/or 9.5 dpc through oral gavage needles at a final concentration of 2 mg/kg of body weight.

Skeleton preparation

E17.5, E18.5, or newborn pups were subjected to skeleton preparations as previously described (Lee et al., 2006). Mice were eviscerated and left in water overnight with gentle shaking. After further removal of skin, fat, muscle, and glands, the sample was fixed in 95% ethanol for 2 to 5 days. The sample was then stained overnight in Alcian blue 8GX staining solution (0.15 mg/ml in 80% ethanol and 20% glacial acetic acid), and rinsed with 95% ethanol. After the tissue debris was cleared in 2% KOH solution for 3 hr, the skeleton was stained with 0.005% alizarin red S in 2% KOH for 3 h. The stained skeleton was rinsed with 2% KOH and kept in 50% glycerol/PBS.

Whole-mount X-gal staining

To detect RA activities in E9.5 or E10.5 embryos, whole-mount X-gal staining was carried out as described previously (Joo et al., 2007). Briefly, collected embryos were fixed in fixing solution (1% formaldehyde, 0.2% glutaraldehyde, 2 mM $MgCl_2$, 5 mM EGTA, 0.02% NP-40 in PBS), rinsed three times with PBS, and stained in X-gal staining solution [5 mM $K_3Fe(CN)_6$, 5 mM $K_4Fe(CN)_6$, 2 mM $MgCl_2$, 0.01% Deoxycholate sodium salt, 0.02% NP-40, 0.75 mg/ml X-gal in 100 mM phosphate buffer (pH7.3)] at 37 °C overnight. Stained embryos were post-fixed in post-fixing solution (4% paraformaldehyde, 0.1% Tween 20 in PBS) at 4 °C overnight.

Whole-mount in situ hybridization

For studying the expression patterns of *MesP2*, *Aldh1a2*, *Gdf11*, *Cyp26a1*, *Fgf8*, and *Wnt3a* in E9.0, E9.5 or E10.5 embryos, antisense RNA probes were produced by using a digoxigenin-UTP labeling kit (Roche Diagnostics Corporation, Indianapolis, IN). The *MesP2* (Saga et al., 1997), *Aldh1a2* (Niederreither et al., 1997), *Gdf11* (McPherron et al., 1999), and *Fgf8* (Mahmood et al., 1995) probes were generated from the template DNAs as described previously. The *Cyp26a1* and *Wnt3a* probes were obtained from *Cyp26a1* EST clone (IMAGE clone No.:6334777) and *Wnt3a* cDNA (NM_009522, nt1180-2266), respectively. Whole-mount *in situ* hybridization was performed as previously described (Wilkinson, 1992). Genomic DNA isolated from yolk sac was used for genotyping embryos.

Results and discussion

Acvr2b and Gdf11 mutants are sensitive to exogenous RA treatment

Exposure of embryos to all-trans RA at a high dose (100 mg/kg bw) at 8.5 dpc has been shown to induce anterior transformations of vertebrae, resulting in C7/T14/L6 or C7/T15/L5 patterns with varied degrees of tail truncation (Kessel and Gruss, 1991; Kessel, 1992). We showed previously that RA treatment of *Acvr2b*$^{-/-}$ embryos at 8.5 dpc with a low dose (10 mg/kg bw), which only moderately induces vertebral patterning defects in WT mice, intensified vertebral defects, resulting in a C7/T18/L6 pattern with truncation of tail (Oh and Li, 1997), indicating that mice deficient in ACVR2B signaling are sensitive to exogenous RA exposure. Because the vertebral patterning defect in *Acvr2b*$^{-/-}$ mice (C7T16L6) is milder than that seen in *Acvr2a*$^{+/-}$;*Acvr2b*$^{-/-}$ mice (C7T17L7; Oh et al., 2002), *Gdf11*$^{-/-}$ mice (C7T18L8; McPherron et al., 1999) or *Gdf11*$^{-/-}$;*Mstn*$^{-/-}$ mice (C7T20L8; McPherron et al., 2009), we sought to determine whether RA could have a similar exacerbating effect in embryos with a more severe patterning phenotype.

As shown in Fig. 1, RA increased the extent of transformations in both activin type II receptor compound mutant and *Gdf11*$^{-/-}$ mice. RA-treated *Acvr2a*$^{+/-}$;*Acvr2b*$^{-/-}$ mice had further increases in the number of thoracic vertebrae (up to 20) with severe truncation of lumbar, sacral and caudal vertebrae (Fig. 1A, B). RA treatment of *Gdf11*$^{-/-}$ mice also resulted in increased thoracic vertebral number to T20 with reduced numbers of lumbar vertebrae and no sacral/caudal vertebrae (Fig. 1C, D). The vertebral patterns of the RA-treated *Gdf11*$^{-/-}$ and *Acvr2a*$^{+/-}$;*Acvr2b*$^{-/-}$ mice are remarkably similar to each other and also very similar to those of *Gdf11*$^{-/-}$;*Mstn*$^{-/-}$ mice (McPherron et al., 2009). Interestingly, *Gdf11*$^{+/-}$ mice also showed a higher sensitivity to the RA treatment compared to their WT littermates. RA treatment (10 mg/kg bw) caused typical thoracolumbar transformations in both *Gdf11*$^{+/+}$ and *Gdf11*$^{+/-}$ mice, but at a higher frequency in *Gdf11*$^{+/-}$ mice (19/20) compared to *Gdf11*$^{+/+}$ mice (6/17). Moreover, RA reduced the number of caudal vertebrae by about 3 in *Gdf11*$^{+/+}$ mice (untreated vs. treated: 28 ± 2 vs. 25 ± 7) compared to about 13 in *Gdf11*$^{+/-}$ mice (30 ± 2 vs. 17 ± 8).

These results clearly demonstrate that mice deficient in GDF11-ACVR2 signaling are sensitive to exogenous RA exposure. Phenotypic overlap (i.e. severe caudal truncation and anterior transformation) among *Gdf11*$^{-/-}$;*Mstn*$^{-/-}$ mice (McPherron et al., 2009), high dose RA-treated WT embryos (Kessel, 1992), and low dose RA treated *Acvr2a/b* and *Gdf11* mutants (Fig. 1) suggested a mechanistic link between RA and GDF/ACVR2 signaling for vertebral patterning and tail development.

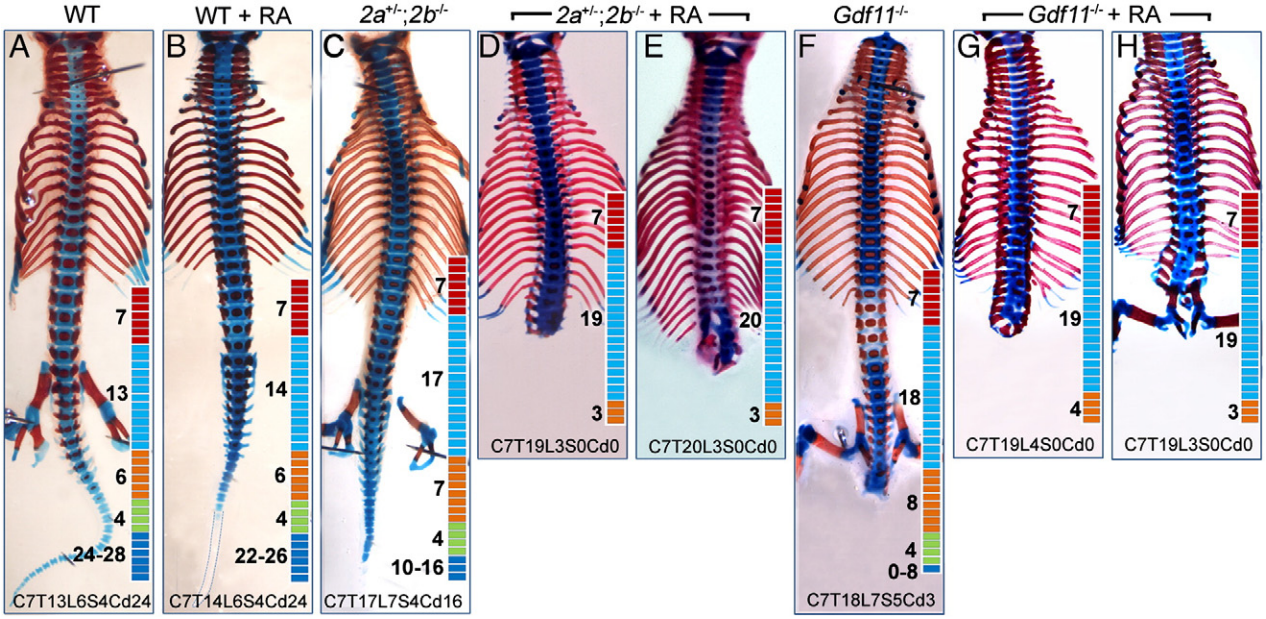

Fig. 1. *Acvr2a/b* and *Gdf11* mutants are sensitive to exogenous RA exposure. Representative ventral view of axial skeletons of wild-type (A, B), *Acvr2a*$^{+/-}$;*Acvr2b*$^{-/-}$ (C–E), and *Gdf11*$^{-/-}$ (F–H) fetuses exposed to either sesame oil (A, C, F) or RA (B, D, E, G, H) *in utero* at 8.5 dpc (10 mg/kg of body weight). Limbs were removed during skeleton preparation. Diagram with colored boxes in each panel indicate a represented number of cervical (C; red), thoracic (T; blue), lumbar (L; orange), sacral (S; green), and caudal (Cd; dark blue) vertebrae. Severe truncations of the axial skeletons occurred posterior to mid-lumbar region in RA exposed *Acvr2* mutants and *Gdf11*$^{-/-}$ fetuses.

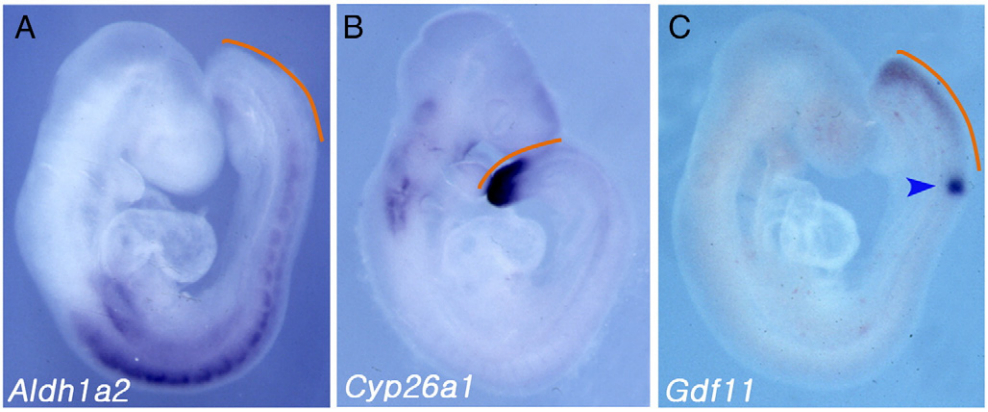

Fig. 2. Gdf11 expression domain overlaps with Cyp26a1 expression in the PSM region. Whole mount *in situ* hybridization of Aldh1a2 (A), Cyp26a1 (B), and Gdf11 (C) in wild-type embryos at E9.0–E9.5 revealed that Gdf11 expression in the PSM region (indicated by orange lines) overlaps with Cyp26a1 but mutually exclusive with Aldh1a2 expression. MesP2 expression is indicated by an arrow head (C).

Cyp26a1 expression is diminished in the PSM region of Gdf11-null embryos

RA levels along the AP axis are tightly regulated by specific distribution of both RA-synthesizing and RA-inactivating enzymes. During critical stages of somitogenesis for thoracic and lumbar vertebral development (E8.5-E10.5), the RA-synthesizing enzyme, ALDH1A2 (aldehyde dehydrogenase family 1 subfamily A2), is predominantly expressed in somites and lateral plate mesoderm but not in the presomitic and tailbud region (Fig. 2A) (Niederreither et al., 1997). Conversely, the RA-inactivating enzyme, CYP26A1, is expressed predominantly in the presomitic and tail bud region (Fig. 2B) (Sakai et al., 2001). This reciprocal expression pattern of RA-synthesizing and -inactivating enzymes may generate a gradient of RA activity along the AP axis, with diminishing RA levels toward the caudal end. The expression domain of Cyp26a1 overlaps with that of Gdf11, which is expressed in the tail bud and the PSM but not in mature somites (Fig. 2C) (Andersson et al., 2006; Nakashima et al., 1999). We investigated whether the Cyp26a1 expression is affected in *Gdf11*$^{-/-}$ embryos at the caudal region by whole mount *in situ* hybridization (WISH) on E9.5 and E10.5 WT and *Gdf11*$^{-/-}$ embryos using a Cyp26a1 anti-sense probe. As shown in Fig. 3G, Cyp26a1 transcripts were reduced and detected only at the tail tip region in E9.5 *Gdf11*$^{-/-}$ embryos. A similar pattern with a more dramatic difference of expression level was observed in E10.5 *Gdf11*$^{-/-}$ embryos in comparison with their WT littermates (Fig. 3B, H). A number of reports have shown that expression of Fgf8 or Wnt3a, important regulators of the somitogenesis, segmentation clock and caudal development, is repressed in the tail bud region of *Cyp26a1*$^{-/-}$ embryos (Abu-Abed et al., 2001, 2003; Baker et al., 2006; Gregg, 2007; Sakai et al., 2001). To determine whether the expression levels of these genes were also affected in *Gdf11*$^{-/-}$ embryos, we performed WISH using *Fgf8* and *Wnt3a* anti-sense probes. The *Wnt3a* expression appeared to be slightly reduced in E9.5 and markedly diminished in E10.5 *Gdf11*$^{-/-}$ embryos (Fig. 3I, J). However, the level of *Fgf8* expression did not appear to be significantly affected in E9.5 and E10.5 *Gdf11*$^{-/-}$ embryos (Fig. 3K, L).

In vivo RA activity gradient is altered in Gdf11-null embryos

To investigate whether the reduced and posteriorly shifted Cyp26a1 expression domain in *Gdf11*$^{-/-}$ embryos affects RA activity along the AP axis in *Acvr2b* and *Gdf11* mutants, we examined the *in vivo* RA activity in *Acvr2b*$^{-/-}$, *Gdf11*$^{-/-}$, and control embryos using

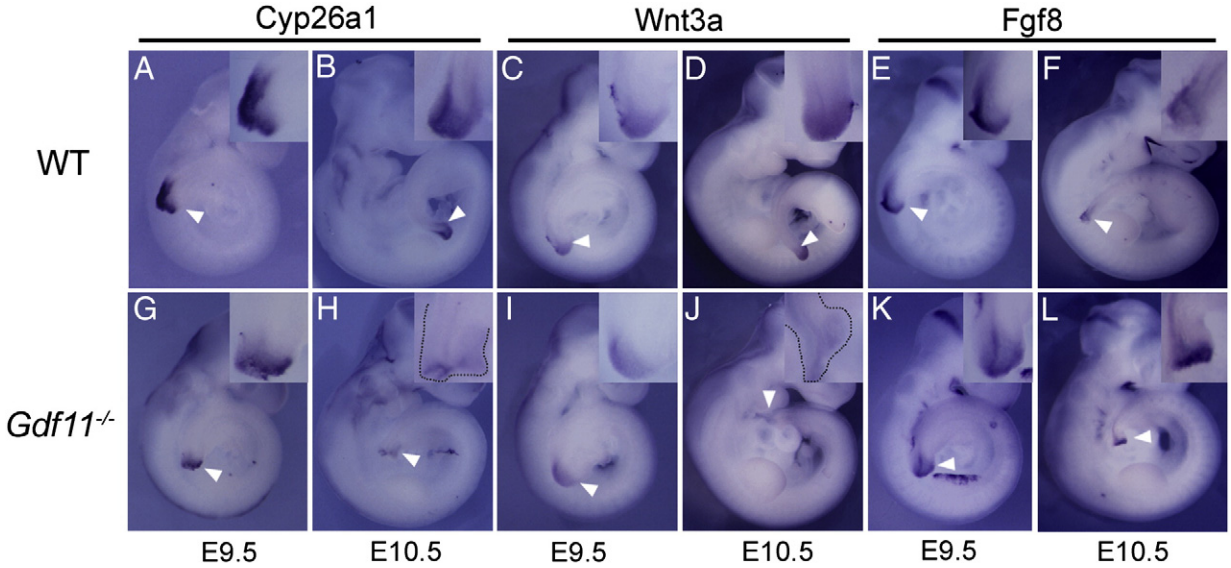

Fig. 3. Altered expression of Cyp26a1 and Wnt3a in *Gdf11*$^{-/-}$ embryos. Whole-mount *in situ* hybridization on E9.5 and E10.5 of WT (A–F) and *Gdf11*$^{-/-}$ (G–L) embryos using antisense-Cyp26a1, -Wnt3a, and -Fgf8 probes. Insets are the magnified views of the PSM/tailbud area. Note the reduced expression of Cyp26a1 and Wnt3a in the tail bud (arrowhead) regions of *Gdf11*$^{-/-}$ embryos.

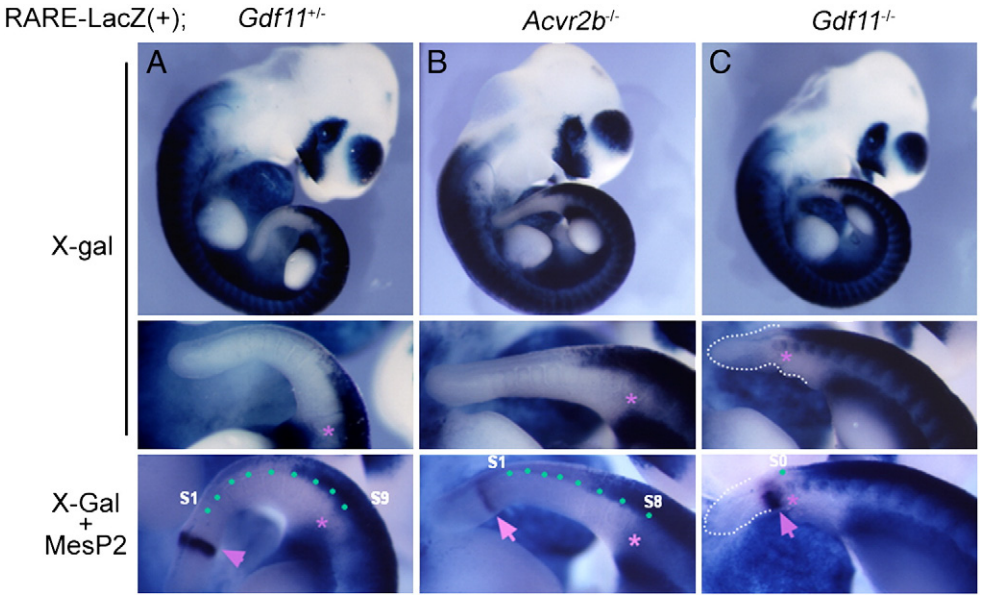

Fig. 4. Posteriorized RA activities in the caudal region of the *Gdf11*$^{-/-}$ embryos. RA activities were visualized by X-gal staining in RARE-LacZ(+);*Gdf11*$^{+/-}$ (A), RARE-LacZ(+);*Acvr2b*$^{-/-}$ (B), and RARE-LacZ(+);*Gdf11*$^{-/-}$ (C) E10.5 embryos. Lower panels are magnified views of posterior regions of the corresponding embryo. Asterisks and arrows indicate the posterior-most X-gal positive somite and MesP2 expression, respectively. MesP2 marks for the junction between the posterior-most somite and the PSM region.

a RA reporter line (*RARE-lacZ*-transgenic mice) in which *LacZ* expression is regulated by retinoic acid response elements (RARE) (Rossant et al., 1991). E10.5 control and mutant embryos were stained with X-gal followed by WISH with an *MesP2* anti-sense probe (Takahashi et al., 2000) to visualize the junction between the PSM and the first mature somite (S0). In WT, *Acvr2b*$^{+/-}$, and *Gdf11*$^{+/-}$ embryos, the posterior-most X-gal positive somite was found on 9th, 10th, or 11th mature somite (S9-S11) (Fig. 4A). The RA activity domain in *Acvr2b*$^{-/-}$ embryos was extended slightly posteriorly compared to that in WT embryos, in which the posterior-most X-gal positive somite was detected on S7-S8 (Fig. 4B). However, a dramatic posterior shift of the RA activity domain was observed in *Gdf11*$^{-/-}$ embryos (Fig. 4C). In most cases, RA activity was detected on S0 near the rostral end of the PSM.

To investigate the timing of this caudal-shift, we examined the pattern of RA activity in earlier stages of WT and *Gdf11*$^{-/-}$ embryos. As shown in Fig. 5A and B, the posterior-most X-gal positive somite was found at S1 in both control ($n=4$) and *Gdf11*$^{-/-}$ embryos ($n=7$) at E9.5. At E10.0, RA activity was undetectable in nascent somites of control embryos, as the posterior-most X-gal positive somite was detected in S4 (Fig. 5C, C'), whereas RA activity was detected in nascent somites of *Gdf11*$^{-/-}$ embryos ($n=2$) (Fig. 5D, D'). These results demonstrate that RA activity is progressively shifted in the anterior direction, (i.e., RA activity is inhibited in nascent somites) in the period between E9.5 and E10.5 in WT embryos, whereas this anterior shift of the RA activity domain did not occur in *Gdf11*$^{-/-}$ embryos. Taken together, these results suggest that down-regulation of Cyp26a1 expression in the PSM region of *Gdf11*$^{-/-}$ embryos

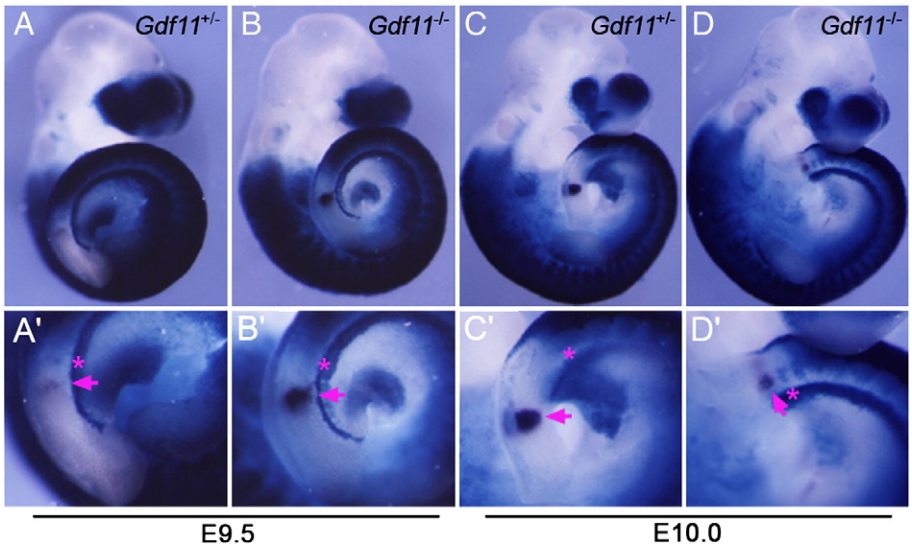

Fig. 5. Impaired inactivation of RA activities in the nascent somites of *Gdf11*$^{-/-}$ embryos during E9.5–E10 stages. RA activities visualized by X-gal staining have no apparent difference between *Gdf11*$^{+/-}$ (A, A') and *Gdf11*$^{-/-}$ (B, B') embryos at E9.5. RA activities were shown to be shifted to the rostral direction in *Gdf11*$^{+/-}$ (C, C') but not in *Gdf11*$^{-/-}$ embryos (D, D') at E10.0. Asterisks and arrows indicate the posterior-most X-gal positive somite and MesP2 expression, respectively.

impairs inactivation of RA activity in nascent somites at E9.5–E10.5 stages, resulting in an expansion of the RA activity domain to the caudal region of *Gdf11*$^{-/-}$ embryos.

Although the RA activity did not appear to be greatly affected in *Acvr2b*$^{-/-}$ embryos (Fig. 4B), we investigated the possibility that the hypersensitivity of *Acvr2b*$^{-/-}$ and *Acvr2a*$^{+/-}$;*Acvr2b*$^{-/-}$ embryos to exogenous RA treatment (Fig. 1) (Oh and Li, 1997) might reflect differences in levels of Cyp26a1 expression in mutant embryos. To test this, we examined the RA activity in E10.5 *Acvr2b*$^{+/-}$ and *Acvr2b*$^{-/-}$ embryos treated with RA at 8.5 dpc. As shown in Fig. 6A, exogenous RA treatment did not alter the RA activity domain in *Acvr2b*$^{+/-}$ or WT (data not shown) embryos. However, the RA treatment shifted the RA activity domain in the posterior direction in *Acvr2b*$^{-/-}$ embryos (Fig. 6C).

Reduced expression or activity of Cyp26a1 affects vertebral patterning

It has been shown that *Cyp26a1*$^{-/-}$ mice display severe truncations of tail vertebrae and a mild vertebral patterning defect represented by a C6T14L5 or C6T15L5 pattern that includes a posterior transformation in the cervicothoracic transition and an anterior transformation in the thoracolumbar transition (Abu-Abed et al., 2001; Sakai et al., 2001). Hence, the vertebral specification defects of *Cyp26a1*$^{-/-}$ mice are very different from those of *Gdf11*$^{-/-}$ mice. Together with our expression data showing that *Cyp26a1* expression is reduced or posteriorly shifted but not absent in *Gdf11*$^{-/-}$ embryos (Fig. 3G, H), these findings suggested that the vertebral phenotype in *Gdf11*$^{-/-}$ mice may in part be due to dysregulation rather than complete repression of Cyp26a1. In order to investigate whether a reduction in expression or activity of CYP26A1 can affect vertebral patterning and/or development of tail vertebrae, we employed both genetic and pharmacological approaches.

The vertebral phenotype of *Acvr2b*$^{-/-}$ mice is sensitive to additional mutation of genes in the same or counteracting signaling pathway and can be either alleviated or intensified depending on further inhibition of BMP or GDF11 signaling, respectively (Andersson et al., 2006; Oh et al., 2002; Park et al., 2004). Therefore, we examined possible genetic interactions between *Acvr2b* and *Cyp26a1* by comparing the vertebral patterns of *Acvr2b*$^{-/-}$;*Cyp26a1*$^{+/-}$ newborn pups with those of *Acvr2b*$^{-/-}$ and *Acvr2b*$^{+/-}$;*Cyp26a1*$^{+/-}$ littermates (Supplemental Fig. 1). Out of nine litters, we have obtained eight *Acvr2b*$^{+/-}$;*Cyp26a1*$^{+/-}$, nine *Acvr2b*$^{-/-}$, and ten *Acvr2b*$^{-/-}$;*Cyp26a1*$^{+/-}$ mice. All eight double heterozygous pups and eight out of nine *Acvr2b*$^{-/-}$ pups exhibited the normal C7T13L6 pattern and the typical C7T16L6 pattern, respectively. Six out of ten *Acvr2b*$^{-/-}$;*Cyp26a1*$^{+/-}$ pups, however, exhibited partial lumbar to thoracic transformation at V24 and therefore exhibited a C7T17(s)L5 pattern.

As an alternative approach, we attempted to reduce the CYP26A1 activity by administering a pharmacological inhibitor of CYP26 enzymes, R115866 (Johnson & Johnson Co). It has been shown that oral administration of this compound into rats can alter levels of RA signaling *in vivo* (Stoppie et al., 2000). It has never been tested, however, whether this compound can efficiently inhibit Cyp26 enzymes in embryos and whether such inhibition would affect vertebral patterning. We first examined the effect of administering the drug to WT pregnant dams at 8.5 dpc via oral gavage in various concentrations ranging from 2.5 to 20 mg/kg of bw. At 20 mg/kg bw, all nine fetuses exhibited cleft palate and small mandible, and some also exhibited an opened-eye phenotype (data not shown). Interestingly, seven out of nine exhibited mild anterior transformation of vertebrae, such as C7T14L6 ($n=3$), C7T14L5 ($n=3$), or C7T14(s)L5 ($n=1$) (Supplemental Fig. 2A, B).

In order to test the impact of this CYP26 inhibitor on *Acvr2b*$^{-/-}$ background, we analyzed the vertebral patterns of E18.5 fetuses treated with the drug (10 mg/kg bw) at 8.5 dpc. At this dosage, none of the WT and *Acvr2b*$^{+/-}$fetuses ($n=7$) exhibited vertebral defects (Supplemental Fig. 2C), whereas *Acvr2b*$^{-/-}$ fetuses displayed more exaggerated vertebral transformation defects in comparison with the unexposed *Acvr2b*$^{-/-}$ mice (Supplemental Fig. 2D, E). One of treated mice was found dead and exhibited the C7T18L4 pattern with a severe truncation of tail vertebrae (Supplemental Fig. 2E). These genetic and pharmacological data provide further support for our model that dysregulation of RA homeostasis mediated by CYP26A1 is an important contributing factor for the axial vertebral defects observed in *Acvr2b*$^{-/-}$ and *Gdf11*$^{-/-}$ mice.

Elevated RA activity is partially responsible for axial vertebral defects in Gdf11-null mice

RA signaling is mediated by retinoic acid receptors (RARA, RARB, and RARG) and retinoid X receptors (RXRA, RXRB, and RXRG) (Mark et al., 2009). It has been shown that RARG is the crucial gene for axial

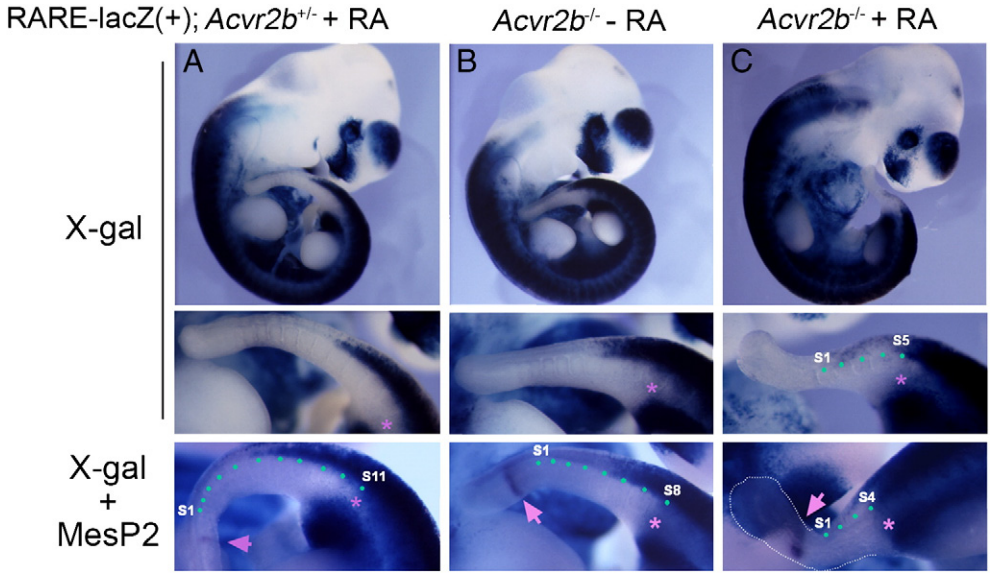

Fig. 6. RA activities of the *Acvr2b*$^{-/-}$ embryos are sensitive to exogenous RA exposure. *In vivo* RA activities of RA-treated RARE-lacZ(+);*Acvr2b*$^{+/-}$ (A), vehicle-treated RARE-lacZ(+);*Acvr2b*$^{-/-}$ (B), and RA-treated RARE-lacZ(+);*Acvr2b*$^{-/-}$ (C) E10.5 embryos exposed to RA (or vehicle) at 8.5 dpc were visualized by X-gal staining followed MesP2 *in situ* hybridization. Asterisks and arrows in the low panels indicate the posterior-most X-gal positive somite and *MesP2* expression, respectively. Green dots indicate the segmented somites.

vertebral development. Rarg is expressed in the tail bud and the PSM, and *Rarg*-deletion has been shown to rescue the vertebral defects of *Cyp26a1*$^{-/-}$ mutants (Abu-Abed et al., 2003). In order to evaluate the extent to which impaired RA homeostasis affects the vertebral defects in *Gdf11*$^{-/-}$ mice, we attempted to block the RA signaling using a pan retinoic acid receptor antagonist, AGN193109 (Johnson et al., 1995; Agarwal et al., 1996). We analyzed axial skeletons of E18.5 WT and *Gdf11*$^{-/-}$ fetuses treated with AGN193109 at 8.5 and/or 9.5 dpc, a crucial developmental period for vertebral specification and tail development. Most WT embryos treated with vehicle or AGN193109 (oral administration, 2 mg/kg of bw) at 8.5 dpc exhibited the normal vertebral pattern (C7T13L6) and had 24–29 caudal vertebrae (average: 27 caudal vertebrae; Fig. 7A; Supplemental Fig. 3A, B). Although the posterior transformation phenotype at the cervicothoracic junction was unaffected, treatment with the drug could almost completely rescue the caudal defects of *Cyp26a1*$^{-/-}$ mutants (Fig. 7B; Supplemental Fig. 3C, D), demonstrating the effectiveness of this regimen. Vehicle-treated *Gdf11*$^{-/-}$ embryos showed typical

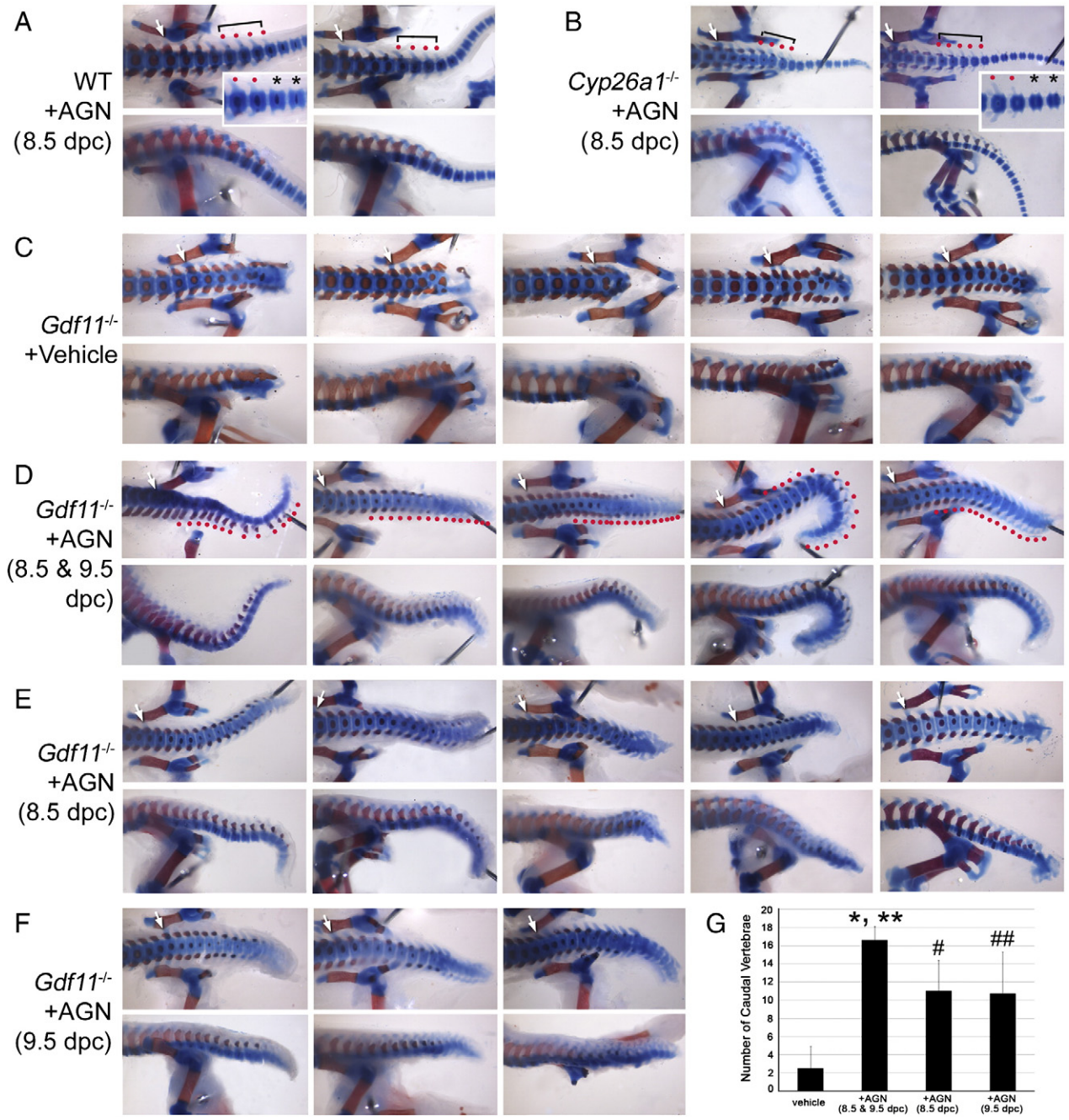

Fig. 7. Tail truncation defects of *Gdf11*$^{-/-}$ mice are significantly rescued by a pan retinoic acid receptor antagonist, AGN193109 (AGN). Representative ventral (upper panels) and lateral (lower panels) views of posterior lumbar, sacral, and proximal caudal vertebrae are shown. All skeletons were collected from E18.5 fetuses, except for *Cyp26a1*$^{-/-}$ from E17.5 (B). White arrows indicate the first sacral vertebra. (A) WT treated with AGN. Red dots with a bracket indicate proximal caudal vertebrae having transverse and spinous processes. Asterisks indicate caudal vertebrae that do not contain transverse and spinous processes. (B) AGN-treated *Cyp26a1*$^{-/-}$ skeletons. AGN treatment almost completely rescued the caudal agenesis defect of *Cyp26a1*$^{-/-}$ fetuses. The morphological transition in the caudal vertebrae is also restored (inset). (C) Vehicle-treated *Gdf11*$^{-/-}$ skeletons. (D) *Gdf11*$^{-/-}$ skeletons treated with AGN for two consecutive days at 8.5 and 9.5 dpc. AGN-treated *Gdf11*$^{-/-}$ embryos show elongated tail. Take notice that the extended caudal vertebrae contain transverse and spinous processes (indicated by red dots). (E, F) *Gdf11*$^{-/-}$ skeletons treated with AGN at 8.5 dpc (E) and 9.5 dpc (F). (G) Histogram showing the number of caudal vertebrae, defined as vertebral segments present posterior to 4th sacral vertebra. Means and standard deviations are shown as filled box and bar above each box, respectively. * ($p<0.0001$), # ($p<0.001$), and ## ($p<0.01$): compared with vehicle-treated *Gdf11*$^{-/-}$ embryos as determined by Student's *t* test. ** ($p<0.05$) compared with AGN-treated *Gdf11*$^{-/-}$ embryos at 8.5 or 9.5 dpc.

C7T18L8 or C7T18L7 patterns with truncation of tails (average: 2.5 caudal vertebrae; Fig. 7C; Supplemental Fig. 3E, F). The treatment of AGN193109 for two consecutive days at 8.5 and 9.5 dpc markedly rescued the tail truncation defect of *Gdf11*$^{-/-}$ fetuses (average: 16.6 caudal vertebrae; Fig. 7D; Supplemental Fig. 3G–I). Drug treatment at either 8.5 or 9.5 dpc could also rescue the tail truncation defect of *Gdf11*$^{-/-}$ but to a less extent than that seen with the 2-day treatment (average: 11 caudal vertebrae; Fig. 7E, F). The effect by the RA signaling inhibitor in terms of rescuing the anterior transformation phenotype of *Gdf11*$^{-/-}$ mice was not as dramatic as that seen in terms of rescuing the tail defect, with the number of thoracic vertebrae being reduced to 17 with 2 days of drug treatment (Supplemental Fig. 3G–I). We did not include the number of lumbar vertebrae for comparison because it was difficult to identify the first sacral vertebra to accurately count the number of lumbar vertebrae.

Gdf11$^{-/-}$ mice display defects in development of axial vertebrae, characterized by severe anterior vertebral transformation and agenesis of caudal vertebrae. Here we have demonstrated that regulation of RA metabolism by CYP26A1 in the PSM/tailbud region is a key downstream mechanism by which GDF11 signaling controls the development of caudal vertebrae. Specifically, we showed that *Gdf11*$^{-/-}$ embryos have diminished expression of Cyp26a1 in the tail bud region and impaired inactivation of RA in nascent somites at E9.5 and E10.5 and that diminished levels of CYP26A1 also correlates with hyper-sensitivity of *Acvr2a/b* and *Gdf11* mutant mice to exogenous RA exposure. Furthermore, we showed that treatment of embryos with a RARG antagonist could rescue the caudal agenesis phenotype of *Gdf11*$^{-/-}$ mice. Interestingly, the RARG antagonist rescued truncation of caudal vertebrae of *Gdf11*$^{-/-}$ mice, but the morphology of the rescued caudal vertebrae was abnormal. In WT mice, a morphological transition (i.e., absence of transverse and spinous processes) occurs at the 5th or 6th caudal vertebra (Fig. 7A inset). Such a transition was present in the rescued caudal vertebrae of *Cyp26a1*$^{-/-}$ mice (Fig. 7B inset) but not in those of *Gdf11*$^{-/-}$ mice (Fig. 7D–F). Although additional studies will be required to determine the extent to which other downstream mediators are required for correct specification of caudal vertebrae, the data presented here strongly suggest that Cyp26a1 is an essential downstream target of GDF11-ACVR2 signaling and that dysregulation of RA metabolism is at least partially responsible for the patterning defects seen in Gdf11 mutant mice. Hence, our studies are consistent with a direct relationship between the pathways regulated by GDF11 and by retinoic acid in establishing positional identity along the anterior-posterior axis and raise the possibility that these signaling pathways may also interact in regulating other developmental processes.

Acknowledgments

We thank Hiroshi Hamada and Janet Rossant for *Cyp26a1*-knockout mice and RARE-LacZ-transgenic mice, respectively. The MesP2, Aldh1a2, Wnt3A and Fgf8 probes were kindly provided by Jung Yun, Karen Niederreither, Andrew McMahon, and Martin Cohn, respectively. This work was supported in part by World Class University (WCU by Korean Ministry of Education, Science and Technology) to S.P.O, and by NIH HD35887/AR060636 to S.J.L.

Appendix A. Supplementary data

Supplementary data to this article can be found online at doi:10.1016/j.ydbio.2010.08.022.

References

Abu-Abed, S., Dolle, P., Metzger, D., Beckett, B., Chambon, P., Petkovich, M., 2001. The retinoic acid-metabolizing enzyme, CYP26A1, is essential for normal hindbrain patterning, vertebral identity, and development of posterior structures. Genes Dev. 15, 226–240.

Abu-Abed, S., Dolle, P., Metzger, D., Wood, C., MacLean, G., Chambon, P., Petkovich, M., 2003. Developing with lethal RA levels: genetic ablation of Rarg can restore the viability of mice lacking Cyp26a1. Development 130, 1449–1459.

Agarwal, C., Chandraratna, R.A.S., Johnson, A.T., Rorke, E.A., Eckert, R.L., 1996. AGN193109 is a highly effective agonist of retinoid action in human ectocervical epithelial cells. J. Biol. Chem. 271, 12209–12212.

Akasaka, T., van Lohuizen, M., van der Lugt, N., Mizutani-Koseki, Y., Kanno, M., Taniguchi, M., Vidal, M., Alkema, M., Berns, A., Koseki, H., 2001. Mice doubly deficient for the Polycomb Group genes Mel18 and Bmi1 reveal synergy and requirement for maintenance but not initiation of Hox gene expression. Development 128, 1587–1597.

Allan, D., Houle, M., Bouchard, N., Meyer, B.I., Gruss, P., Lohnes, D., 2001. RARgamma and Cdx1 interactions in vertebral patterning. Dev. Biol. 240, 46–60.

Andersson, O., Reissmann, E., Ibanez, C.F., 2006. Growth differentiation factor 11 signals through the transforming growth factor-beta receptor ALK5 to regionalize the anterior–posterior axis. EMBO Rep. 7, 831–837.

Baker, R.E., Schnell, S., Maini, P.K., 2006. A clock and wavefront mechanism for somite formation. Dev. Biol. 293, 116–126.

Carapuco, M., Novoa, A., Bobola, N., Mallo, M., 2005. Hox genes specify vertebral types in the presomitic mesoderm. Genes Dev. 19, 2116–2121.

Core, N., Bel, S., Gaunt, S.J., Aurrand-Lions, M., Pearce, J., Fisher, A., Djabali, M., 1997. Altered cellular proliferation and mesoderm patterning in Polycomb-M33-deficient mice. Development 124, 721–729.

Dichmann, D.S., Yassin, H., Serup, P., 2006. Analysis of pancreatic endocrine development in GDF11-deficient mice. Dev. Dyn. 235, 3016–3025.

Esquela, A.F., Lee, S.J., 2003. Regulation of metanephric kidney development by growth/differentiation factor 11. Dev. Biol. 257, 356–370.

Essalmani, R., Zaid, A., Marcinkiewicz, J., Chamberland, A., Pasquato, A., Seidah, N.G., Prat, A., 2008. In vivo functions of the proprotein convertase PC5/6 during mouse development: Gdf11 is a likely substrate. Proc. Natl. Acad. Sci. 105, 5750–5755.

Gregg, D., 2007. Retinoic acid regulation of the somitogenesis clock. Birth Defects Res. C: Embryo Today: Reviews 81, 84–92.

Johnson, A.T., Klein, E.S., Gillett, S.J., Wang, L.M., Song, T.K., Pino, M.E., Chandraratna, R.A. S., 1995. Synthesis and characterization of a highly potent and effective antagonist of retinoic acid receptors. J. Med. Chem. 38, 4764–4767.

Joo, J.H., Lee, Y.J., Munguba, G.C., Park, S., Taxter, T.J., Elsagga, M.Y., Jackson, M.R., Oh, S.P., Sugrue, S.P., 2007. Role of Pinin in neural crest, dorsal dermis, and axial skeleton development and its involvement in the regulation of Tcf/Lef activity in mice. Dev. Dyn. 236, 2147–2158.

Kessel, M., 1992. Respecification of vertebral identities by retinoic acid. Development 115, 487–501.

Kessel, M., Gruss, P., 1991. Homeotic transformations of murine vertebrae and concomitant alteration of Hox codes induced by retinoic acid. Cell 67, 89–104.

Lee, Y.J., Hong, K.H., Yun, J., Oh, S.P., 2006. Generation of activin receptor type IIB isoform-specific hypomorphic alleles. Genesis 44, 487–494.

Mahmood, R., Bresnick, J., Hornbruch, A., Mahony, C., Morton, N., Colquhoun, K., Martin, P., Lumsden, A., Dickson, C., Mason, I., 1995. A role for FGF-8 in the initiation and maintenance of vertebrate limb bud outgrowth. Curr. Biol. 5, 797–806.

Mallo, M., Vinagre, T., Carapuco, M., 2009. The road to the vertebral formula. Int. J. Dev. Biol. 53, 1469–1481.

Mark, M., Ghyselinck, N.B., Chambon, P., 2009. Function of retinoic acid receptors during embryonic development. Nucl. Recept. Signal. 7, e002.

Massague, J., 1998. TGF-beta signal transduction. Annu. Rev. Biochem. 67, 753–791.

McIntyre, D.C., Rakshit, S., Yallowitz, A.R., Loken, L., Jeannotte, L., Capecchi, M.R., Wellik, D.M., 2007. Hox patterning of the vertebrate rib cage. Development 134, 2981–2989.

McPherron, A.C., Lawler, A.M., Lee, S.J., 1999. Regulation of anterior/posterior patterning of the axial skeleton by growth/differentiation factor 11. Nat. Genet. 22, 260–264.

McPherron, A.C., Huynh, T.V., Lee, S.J., 2009. Redundancy of myostatin and growth/differentiation factor 11 function. BMC Dev. Biol. 9, 24.

Nakashima, M., Toyono, T., Akamine, A., Joyner, A., 1999. Expression of growth/differentiation factor 11, a new member of the BMP/TGF[beta] superfamily during mouse embryogenesis. Mech. Dev. 80, 185–189.

Niederreither, K., McCaffery, P., Drager, U.C., Chambon, P., Dolle, P., 1997. Restricted expression and retinoic acid-induced downregulation of the retinaldehyde dehydrogenase type 2 (RALDH-2) gene during mouse development. Mech. Dev. 62, 67–78.

Nowicki, J.L., Burke, A.C., 2000. Hox genes and morphological identity: axial versus lateral patterning in the vertebrate mesoderm. Development 127, 4265–4275.

Oh, S.P., Li, E., 1997. The signaling pathway mediated by the type IIB activin receptor controls axial patterning and lateral asymmetry in the mouse. Genes Dev. 11, 1812–1826.

Oh, S.P., Yeo, C.Y., Lee, Y., Schrewe, H., Whitman, M., Li, E., 2002. Activin type IIA and IIB receptors mediate Gdf11 signaling in axial vertebral patterning. Genes Dev. 16, 2749–2754.

Park, S., Lee, Y.J., Lee, H.J., Seki, T., Hong, K.H., Park, J., Beppu, H., Lim, I.K., Yoon, J.W., Li, E., Kim, S.J., Oh, S.P., 2004. B-cell translocation gene 2 (Btg2) regulates vertebral patterning by modulating bone morphogenetic protein/smad signaling. Mol. Cell. Biol. 24, 10256–10262.

Pearlmann, T., 2002. Retinoid metabolism: a balancing act. Nat. Genet. 31, 7–8.

Rossant, J., Zirngibl, R., Cado, D., Shago, M., Giguere, V., 1991. Expression of a retinoic acid response element-hsplacZ transgene defines specific domains of transcriptional activity during mouse embryogenesis. Genes Dev. 5, 1333–1344.

Saga, Y., Takeda, H., 2001. The making of the somite: molecular events in vertebrate segmentation. Nat. Rev. Genet. 2, 835–845.

Saga, Y., Hata, N., Koseki, H., Taketo, M.M., 1997. Mesp2: a novel mouse gene expressed in the presegmented mesoderm and essential for segmentation initiation. Genes Dev. 11, 1827–1839.

Sakai, Y., Meno, C., Fujii, H., Nishino, J., Shiratori, H., Saijoh, Y., Rossant, J., Hamada, H., 2001. The retinoic acid-inactivating enzyme CYP26 is essential for establishing an uneven distribution of retinoic acid along the anterio-posterior axis within the mouse embryo. Genes Dev. 15, 213–225.

Seidah, N.G., Mayer, G., Zaid, A., Rousselet, E., Nassoury, N., Poirier, S., Essalmani, R., Prat, A., 2008. The activation and physiological functions of the proprotein convertases. Int. J. Biochem. Cell Biol. 40, 1111–1125.

Song, J., Oh, S.P., Schrewe, H., Nomura, M., Lei, H., Okano, M., Gridley, T., Li, E., 1999. The type II activin receptors are essential for egg cylinder growth, gastrulation, and rostral head development in mice. Dev. Biol. 213, 157–169.

Stoppie, P., Borgers, M., Borghgraef, P., Dillen, L., Goossens, J., Sanz, G., Szel, H., Van Hove, C., Van Nyen, G., Nobels, G., Vanden Bossche, H., Venet, M., Willemsens, G., Van Wauwe, J., 2000. R115866 inhibits all-trans-retinoic acid metabolism and exerts retinoidal effects in rodents. J. Pharmacol. Exp. Ther. 293, 304–312.

Szumska, D., Pieles, G., Essalmani, R., Bilski, M., Mesnard, D., Kaur, K., Franklyn, A., El Omari, K., Jefferis, J., Bentham, J., Taylor, J.M., Schneider, J.E., Arnold, S.J., Johnson, P., Tymowska-Lalanne, Z., Stammers, D., Clarke, K., Neubauer, S., Morris, A., Brown, S.D., Shaw-Smith, C., Cama, A., Capra, V., Ragoussis, J., Constam, D., Seidah, N.G., Prat, A., Bhattacharya, S., 2008. VACTERL/caudal regression/Currarino syndrome-like malformations in mice with mutation in the proprotein convertase Pcsk5. Genes Dev. 22, 1465–1477.

Takahashi, Y., Koizumi, K., Takagi, A., Kitajima, S., Inoue, T., Koseki, H., Saga, Y., 2000. Mesp2 initiates somite segmentation through the Notch signalling pathway. Nat. Genet. 25, 390–396.

van den Akker, E., Forlani, S., Chawengsaksophak, K., de Graaff, W., Beck, F., Meyer, B.I., Deschamps, J., 2002. Cdx1 and Cdx2 have overlapping functions in anteroposterior patterning and posterior axis elongation. Development 129, 2181–2193.

Wellik, D.M., 2007. Hox patterning of the vertebrate axial skeleton. Dev. Dyn. 236, 2454–2463.

Wellik, D.M., Capecchi, M.R., 2003. Hox10 and Hox11 genes are required to globally pattern the mammalian skeleton. Science 301, 363–367.

White, J.A., Guo, Y.D., Baetz, K., Beckett-Jones, B., Bonasoro, J., Hsu, K.E., Dilworth, F.J., Jones, G., Petkovich, M., 1996. Identification of the retinoic acid-inducible all-trans-retinoic acid 4-hydroxylase. J. Biol. Chem. 271, 29922–29927.

Wilkinson, D.G., 1992. In situ hybridization: a practical approach. Oxford University Press, London, United Kingdom.

Yang, X., Letterio, J.J., Lechleider, R.J., Chen, L., Hayman, R., Gu, H., Roberts, A.B., Deng, C., 1999. Targeted disruption of SMAD3 results in impaired mucosal immunity and diminished T cell responsiveness to TGF-beta. EMBO J. 18, 1280–1291.